Reactivity of the Verdoheme Analogues, 5-Oxaporphyrin Complexes of Cobalt(II) and Zinc(II), with Nucleophiles: Opening of the Planar Macrocycle by Alkoxide Addition To Form Helical Complexes†

Lechosław Latos-Grażyński,‡ James Johnson,§ Saeed Attar,§ Marilyn M. Olmstead,§ and Alan L. Balch*,§

Departments of Chemistry, University of California, Davis, California 95616, and University of Wrocław, Wrocław, Poland

Received December 17, 1997

The 5-oxaporphyrin macrocycle is a modified porphyrin (with an oxygen atom replacing a *meso*-methine unit) that is produced during heme degradation in biological and chemical systems. We have undertaken an investigation into the chemical reactivity of metal complexes of this macrocycle. Here we report that the diamagnetic zinc(II) and paramagnetic cobalt(II) verdoheme analogues, $[Zn^{II}(OEOP)](O_2CCH_3)$ and $[Co^{II}(OEOP)](PF_6)$ (OEOP is the monoanion of octaethyl-5-oxaporphyrin), undergo ring opening when treated with alkoxide ions. The zinc(II) complex Zn^{II}(OEBOMe), where OEBOMe is the dianion of octaethylmethoxybiliverdin, is sufficiently stable to be isolated in crystalline form, but the cobalt(II) analogue, Co^{II}(OEBOMe), is less stable and has been characterized primarily by ^{1}H NMR spectroscopy in solution. The reactions are accompanied by a color change from blue-green for the verdoheme complexes to yellow-green for the ring-opened compounds. The ring-opened product Zn^{II}(OEBOMe) has been subjected to a crystallographic study which reveals that the complex contains a four-coordinate zinc(II) ion whose geometry is significantly controlled by the helical tetrapyrrole ligand so that tetrahedral coordination is not achieved. The structure of this complex is compared to that of a closely related free ligand and those of copper and cobalt complexes of tetrapyrrole ligands that also form helical complexes.

Introduction

Oxidative destruction of hemes by either heme oxygenase[1,2] or the coupled oxidation process produces verdohemes,[3,45,6] the green iron(II) complexes of the 5-oxaporphyrin macrocycle, **1**.

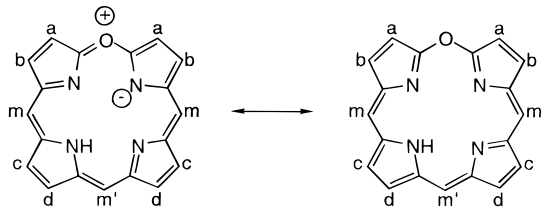

1
5-oxaporphyrin
HOEOP, a, b, c, d = ethyl; m, m' = hydrogen

Although iron,[3−6] cobalt,[7,8] and zinc[9−12] complexes of 5-oxaporphyrins have been prepared, relatively little is known about the reactivity of such complexes. However, it is clear that both metal-centered and ligand-centered reactions can occur. For metal-centered reactions, changes in metal oxidation state as well as changes in axial ligation have been shown to occur for iron[4,5] and cobalt[7,8] complexes without alteration of the 5-oxaporphyrin macrocycle. Additionally, it has been noted that the 5-oxaporphyrin ligand itself can be subject to nucleophilic attack. The products of nucleophilic addition have been formulated as either closed macrocycles, **2**, with the nucleophile

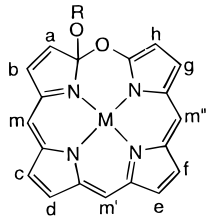

2

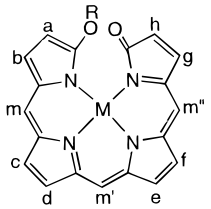

3

attached to the carbon atoms adjacent to the 5-oxa group, or

† Abbreviations used: H_2OEP, octaethylporphyrin; HOEOP, octaethyl-5-oxaporphyrin; H_3OEB, octaethylbilindione; octaethylformylbiliverdin H_2-OEFB; H_2OEBOMe, octaethylmethoxybiliverdin; py, pyridine.

‡ University of Wrocław.

§ University of California.

(1) Maines, M. D. *Heme Oxygenase: Clinical Applications and Functions*; CRC Press: Boca Raton, FL, 1992.
(2) Bissell, D. M. In *Liver: Normal Function and Disease. Bile Pigments and Jaundice*; Ostrow, J. D., Ed.; Marcel Dekker: New York, 1986; Vol. 4, p 133.
(3) Lagarias, J. C. *Biochim. Biophys. Acta* **1982**, *717*, 12.
(4) Balch, A. L.; Latos-Grażyński, L.; Noll, B. C.; Olmstead, M. M.; Szterenberg, L.; Safari, N. *J. Am. Chem. Soc.* **1993**, *115*, 1422.
(5) Balch, A. L.; Noll, B. C.; Safari, N. *Inorg. Chem.* **1993**, *32*, 2901−2905.
(6) Balch, A. L.; Koerner, R.; Olmstead, M. M. *J. Chem. Soc., Chem. Commun.* **1995**, 873−874.
(7) Balch, A. L.; Mazzanti, M.; Olmstead, M. M. *J. Chem. Soc., Chem. Commun.* **1994**, 269.
(8) Balch, A. L.; Mazzanti, M.; St. Claire, T. M.; Olmstead, M. M. *Inorg. Chem.* **1995**, *34*, 2194.
(9) Fuhrhop, J.-H.; Salek, A.; Subramanian, J.; Mengersen, C.; Besecke, S. *Leibigs Ann. Chem.* **1975**, 1131.
(10) Fuhrhop, J.-H.; Krüger, P.; Sheldrick, W. S. *Leibigs Ann. Chem.* **1977**, 339.
(11) Fuhrhop, J.-H.; Krüger, P. *Liebigs Ann. Chem.* **1977**, 360.
(12) Hempenius, M. A.; Koek, J. H.; Lugtenburg, J.; Fokkens, R. *Rec. Trav. Chim. Pays-Bas* **1987**, *106*, 105−112.

S0020-1669(97)01584-X CCC: $15.00
Published on Web 08/13/1998

the open-chain tetrapyrroles, **3**.[9−11] These two structures cannot be readily differentiated through symmetry-based spectroscopic techniques, since both structures contain four distinct pyrrolic rings and three different *meso*-carbon atoms. Consequently, we have undertaken a thorough examination of the products of alkoxide additions to diamagnetic $Zn^{II}(OEOP)^+$ and paramagnetic $Co^{II}(OEOP)^+$ through both spectroscopic and crystallographic techniques. In part these studies were undertaken to provide models for their iron counterparts.[13] Iron complexes of linear tetrapyrroles analogous to **3** are considerably less stable with respect to demetalation than those of other late transition metal ions,[14,15] and we experienced considerable difficulty im characterizing the products of the reaction of verdoheme itself with alkoxide ion. However, we recently have been able to isolate and fully characterize a dimeric iron(II) complex that results from addition of methoxide to $ClFe^{II}(OEOP)$.[13]

Both **2** and **3** represent chiral molecules whose chirality arises from the presence of a tetrasubstituted carbon atom in **2** or a helical arrangement of the open tetrapyrrole in **3** where the overlap of the OR group and the terminal lactam function prevents the molecule from assuming a planar structure. A number of metal complexes of open chain tetrapyrrole ligands that are related to **3** have been studied previously. These include complexes derived from octaethylbilindione, **4** (H_3OEB),[12,16−21]

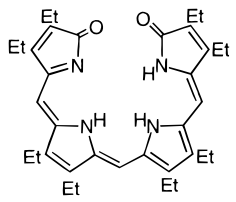

4, (H_3OEB)

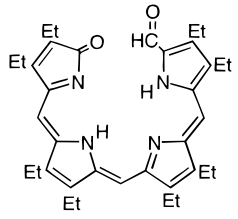

5, (H_2OEFB)

and those derived from octaethylformylbiliverdin, **5** (H_2OEFB).[15] Both of these ligands can produce four-coordinate complexes with helical geometry. Complexes of Cu(II), Ni(II), and Co(II) with octaethylformylbiliverdin, **5** (H_2OEFB), as the ligand behave much like their porphyrin counterparts.[15] However, complexes prepared from octaethylbilindione, **4** (H_3OEB), have unusual electronic structures that frequently exhibit significant ligand radical character.

Results

The diamagnetic zinc(II) and paramagnetic cobalt(II) verdoheme analogues, **6** and **7**, undergo ring opening when treated with alkoxide ions as shown in eq 1. The zinc(II) complex, **8a**,

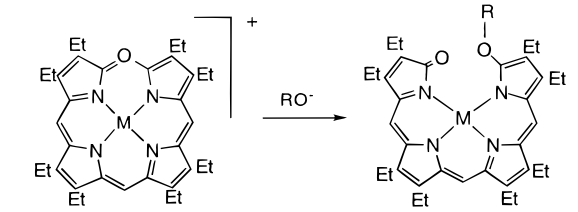

6, M = Zn(II), $[Zn^{II}(OEOP)]^+$

7, M = Co(II), $[Co^{II}(OEOP)]^+$

8a, M = Zn(II), Zn^{II}(OEBOMe)
8b, M = Zn(II), Zn^{II}(OEBOEt)
9a, M = Co(II), Co^{II}(OEBOMe)
9b, M = Co(II), Co^{II}(OEBOEt)

(1)

is sufficiently stable to be isolated in crystalline form, but the cobalt(II) complex, **9a**, is less stable and has been characterized primarily by ^{1}H NMR spectroscopy in solution. The reactions are accompanied by a color change from blue-green for the verdoheme complexes to yellow-green for the ring-opened compounds. Figure 1 compares the electronic absorption spectrum of the verdoheme analogue, $[Zn^{II}(OEOP)](O_2CCH_3)$, with that of the ring-opened product, Zn^{II}(OEBOMe). The spectrum of $[Zn^{II}(OEOP)](O_2CCH_3)$ in trace A shows typical verdoheme-type features with an intense, low-energy absorption at 652 nm, while the spectrum of Zn^{II}(OEBOMe) in trace B shows a much broader and less intense low-energy feature and also a broadened absorption in the region of the Soret band of porphyrins. Similar spectral changes in the UV/vis region are seen for the conversion of $[Co^{II}(OEOP)](PF_6)$ into Co^{II}(OEBOMe) and the spectrum of the product is shown in trace C of Figure 1. The spectrum of Co^{II}(OEBOMe) is similar to that of its zinc analogue, Zn^{II}(OEBOMe).

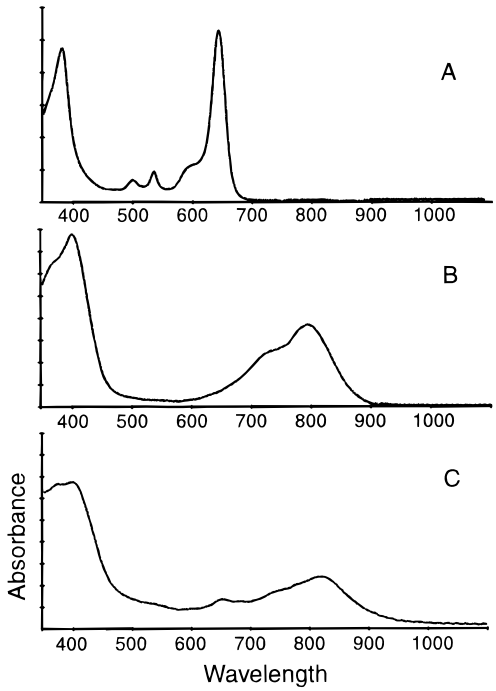

Figure 1. Electronic absorption spectra: (A) $[Zn^{II}(OEOP)](O_2CCH_3)$, **1**, in dichloromethane solution, λ_{max}, nm (ϵ, M^{-1} cm^{-1}) 278 (18 000), 304 (23 000), 334 (24 000), 392 (30 000), 512 (6000), 548 (7000), 612 (7500), 652 (25 000); (B) Zn^{II}(OEBOMe), **3**, in methanol solution, λ_{max}, nm (ϵ, M^{-1} cm^{-1}) 322 (22 300), 402 (33 600), 790 (16 000); (C) Co^{II}(OEBOMe), **4,** in methanol solution, λ_{max}, nm (relative ϵ) 375 (0.99), 400 (1), 823 (0.39).

Crystal and Molecular Structure of Zn^{II}(OEBOMe). The structure of Zn^{II}(OEBOMe) has been studied by X-ray diffrac-

(13) Koerner, R.; Latos-Grażyński, L.; Balch, A. L. *J. Am. Chem. Soc.*, in press.
(14) Balch, A. L.; Latos-Grażyński, L.; Noll, B. C.; Olmstead, M. M.; Safari, N. *J. Am. Chem. Soc.* **1993**, *115*, 9056−9061.
(15) Koerner, R.; Olmstead, M. M.; Ozarowski, A.; Phillips, S. L.; Van Calcar, P. M.; Winkler, K.; Balch, A. L. *J. Am. Chem. Soc.* **1998**, *120*, 1274.
(16) Balch, A. L.; Mazzanti, M.; Noll, B. C.; Olmstead, M. M. *J. Am. Chem. Soc.* **1993**, *115*, 12206−12207.
(17) Balch, A. L.; Mazzanti, M.; Noll, B. C.; Olmstead, M. M. *J. Am. Chem. Soc.* **1994**, *116*, 9114−9122.
(18) Attar, S.; Balch, A. L.; Van Calcar, P. M.; Winkler, K. *J. Am. Chem. Soc.* **1997**, *119*, 3317−3323.
(19) Attar, S.; Ozarowski, A.; Van Calcar, P. M.; Winkler, K.; Balch, A. L. *Chem. Commun.* **1997**, 1115−1116.
(20) Bonnett, R.; Buckley, D. G.; Hamzetash, D. *J. Chem. Soc., Perkin Trans. 1* **1981**, 322.
(21) Bonfiglio, J. V.; Bonnett, R.; Buckley, D. G.; Hamzetash, D.; Hursthouse, M. B.; Malik, K. M. A.; McDonagh, A. F.; Trotter, J. *Tetrahedron* **1983**, *39*, 1865.
(22) Kratky, C.; Jorde, C.; Falk, H.; Thirring, K. *Tetrahedron* **1983**, *39*, 1859.

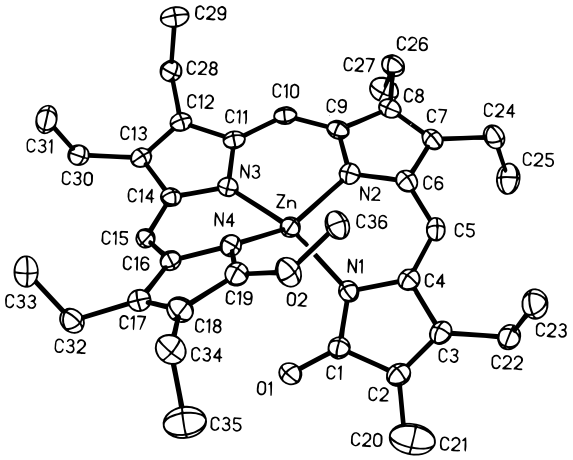

Figure 2. Perspective view of Zn^{II}(OEBOMe) with 50% thermal contours for all non-hydrogen atoms. For clarity, the hydrogen atoms have been omitted.

Table 1. Selected Bond Lengths (Å) and Bond Angles (degree) for Zn^{II}(OEBOMe)

bond lengths		bond angles	
Zn−N(1)	1.976(2)	N(1)−Zn−N(2)	91.83(10)
Zn−N(2)	2.015(3)	N(1)−Zn−N(3)	154.01(10)
Zn−N(3)	1.979(2)	N(1)−Zn−N(4)	101.35(10)
Zn−N(4)	2.102(3)	N(2)−Zn−N(3)	91.97(10)
C(1)−O(1)	1.227(4)	N(2)−Zn−N(4)	146.25(10)
C(19)−O(2)	1.327(4)	N(3)−Zn−N(4)	89.48(10)
O(1)···O(2)	3.580(4)		

tion. A perspective view of the complex is shown in Figure 2. Table 1 contains selected interatomic distances and angles.

The ligand in Zn^{II}(OEBOMe) has a helical geometry which is similar to the ligand orientations in a number of complexes of open chain tetrapyrrole ligands. Relevant examples include Cu^{II}(OEFB), **10**,[15] and Co(OEB), **11**,[16] as well as the free ligand, H_2MeEtBOMe, **12.**[22] There is a center of symmetry in the space group $P\bar{1}$, so the crystal of Zn^{II}(OEBOMe) contains a racemate of the two enantiomeric helices.

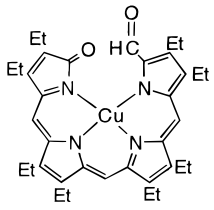

10, Cu^{II}(OEFB)

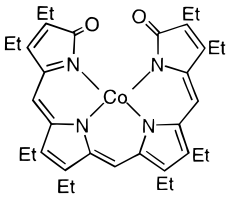

11, Co(OEB)

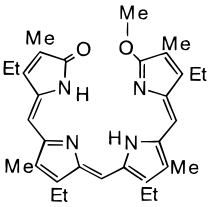

12, (H_2MeEtBOMe)

The zinc ion is four coordinate. The Zn−N(4) distance, 2.102(3) Å, is slightly longer than the other Zn−N distances, which fall in the range 1.975(2)−2.015(3) Å. A similar situation exists in Cu^{II}(OEFB), **10**, where the Cu−N bond that involves the ring with the formyl substituent is somewhat longer than the other three Cu−N bonds. The Zn−N distances are similar to those found in zinc porphyrins, where the bond distances fall in the range 2.06−2.07 Å.[23]

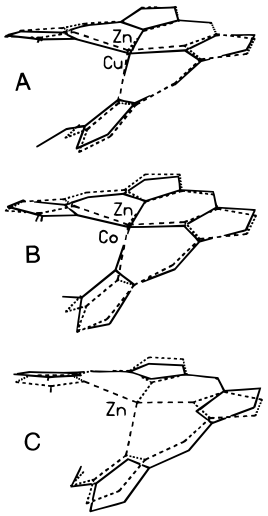

Figure 3. Comparisons of the tetrapyrrole skeletons in (A) Zn^{II}(OEBOMe) (dashed line) and Cu^{II}(OEFB) (solid line), (B) Zn^{II}(OEBOMe) (dashed line) and Co(OEB) (solid line), and (C) Zn^{II}(OEBOMe) (dashed line) and H_2MeEtBOMe (solid line).

The angular disposition of nitrogen atoms about the zinc ion is quite irregular. The three N−Zn−N angles that are internal to a chelate ring (91.97(10), 89.48(10), and 91.83(10)°) are all nearly 90°. The other three are considerably wider, 101.35(10), 146.25(10), and 154.01(10)°. Comparison with Cu^{II}(OEFB), **10**,[15] is instructive, since both complexes involve unsymmetrical, linear tetrapyrrole ligands which are dianions. In Cu^{II}(OEFB) the overlap of the terminal functionalities of the tetrapyrrole ligand prohibit the ligand and the metal ion from assuming a completely planar geometry. On the other hand, in Zn^{II}(OEBOMe) the geometry about the metal appears to be a compromise between the preference for four-coordinate zinc(II) to assume a tetrahedral structure and the requirements of the π-system of the ligand which serve to hold portions of the ligand to a locally planar geometry. The two structures are compared by overlaying one upon the other in part A of Figure 3. Thus in Cu^{II}(OEFB), the pseudotrans angles of 157.65(10) and 158.40(11)° that correspond to N(1)−Zn−N(3) and N(2)−Zn−N(4) angles of 154.01(10) and 146.25(10)° in Zn^{II}(OEBOMe) are wider but not linear. Additionally, the angle that corresponds to the N(1)−Zn−N(4) angle of 101.35(10)° in Zn^{II}(OEBOMe) is narrowed to 95.84(10)° in Cu^{II}(OEFB). Comparison of the nonbonded O···O distance (3.580 Å) in Zn^{II}(OEBOMe) with the nonbonded O···C(formyl) distance (3.544 Å) in Cu^{II}(OEFB) indicates that the two tetrapyrrole ligands have similar helical pitches.

As can be seen by turning to part B of Figure 3, similar considerations pertain when Zn^{II}(OEBOMe) is compared to the somewhat more symmetrical complex Co(OEB), **11**.[16] In the latter complex, the pseudotrans N−Co−N angle (162.0(2)) is closer to linearity than the corresponding N(1)−Zn−N(3) and N(2)−Zn−N(4) angles in Zn^{II}(OEBOMe). Additionally, the nonbonded O···O distance (3.580 Å) in the zinc complex is significantly larger than the corresponding O···O distance (3.116 Å) in Co(OEB).

The structure of Zn^{II}(OEBOMe) can also be compared to that of the related free ligand, H_2MeEtBOMe, **12**.[22] The two

(23) Scheidt, W. R. In *The Porphyrins*; Dolphin, D., Ed.; Academic Press: New York, 1978; Vol. 3, p 463.

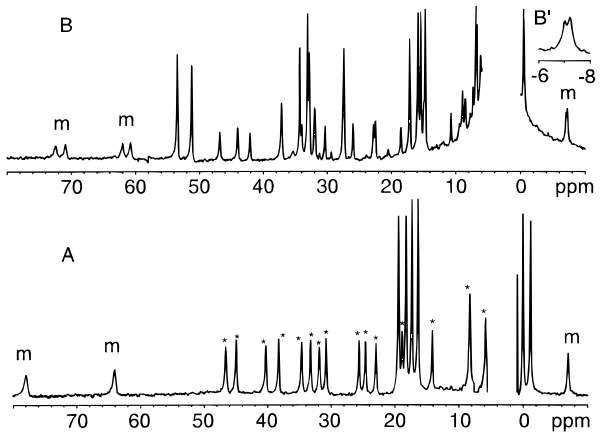

Figure 4. 300 MHz ^{1}H NMR spectra of (A) Co^{II}(OEBOMe-d_4) formed by treating [Co^{II}(OEOP)](PF_6) with potassium hydroxide in methanol-d_4 at 23 °C and (B) Co^{II}(EtioBOMe-d_4) formed by treating [Co^{II}-(EtioOP)](PF_6) with potassium hydroxide in methanol-d_4 at 23 °C. Resonances from the *meso* protons are labeled m, and resonances of the methylene protons are labeled with an asterisk.

structures are compared in part C of Figure 3 where they are overlaid. The free ligand itself has a helical geometry that is similar to that found in the zinc complex. Coordination to zinc results in twisting of the pyrrole rings from their position in the free ligand so that, as expected, they are drawn inward toward the metal ion in the zinc complex.

^{1}H NMR Studies of Alkoxide Addition to [Co^{II}(OEOP)]$^+$. The additions of various alkoxides to [Co^{II}(OEOP)]$^+$ and related Co(II) complexes have been monitored by ^{1}H NMR studies in solution. These spectroscopic results are complicated because the spectra show variations due to changes in concentration and solvent that suggest that axial ligation as well as ligand structure are subject to alteration.

Trace A of Figure 4 shows the ^{1}H NMR spectrum of a sample of [Co^{II}(OEOP)]$^+$ in methanol-d_4 after the addition of potassium hydroxide. A similar spectrum is obtained from the addition of potassium methoxide in methanol-d_4. The spectrum shown in trace A reveals that all of the [Co^{II}(OEOP)]$^+$ (which has *meso* resonances at 30 and 21 ppm, and methylene and methyl resonances in the 8 to −2 ppm range) is consumed and that a new species, Co^{II}(OEBOMe), is present. On the basis of relative intensities and line widths, it is possible to assign these resonances. The three equally intense and slightly broader resonances at 78, 64, and −7 ppm are assigned to the three *meso* protons. As usual for complexes derived from octaethylporphyrin, the *meso* resonances are broadened by their proximity to the paramagnetic center. The resonances labeled with an asterisk in trace A are, with one exception, twice as intense as the *meso* resonances and are assigned to the methylene protons. One of these resonances has twice the intensity of the others, so a total of 15 resonances are resolved. Four equally intense resonances appear in the 20−15 ppm region. These are assigned to the methyl protons. Three other methyl resonances appear in the −2 to 1 ppm region. The fourth methyl resonance is found at 2.5 ppm but is obscured in trace A by a diamagnetic resonance that originates from impurities in the solvent.

Trace B of Figure 4 shows the ^{1}H NMR spectrum that results from the addition of methoxide ion to a solution of [Co^{II}-(EtioOP)]$^+$, **13**, in methanol-d_4. In this case, the unsymmetrical nature of the macrocycle requires the formation of two different products, **14** and **15**, through attack at the two slightly different C−O bonds (one with an adjacent methyl group, one with an adjacent ethyl group) in **13** as shown in eq 2. Thus in trace B

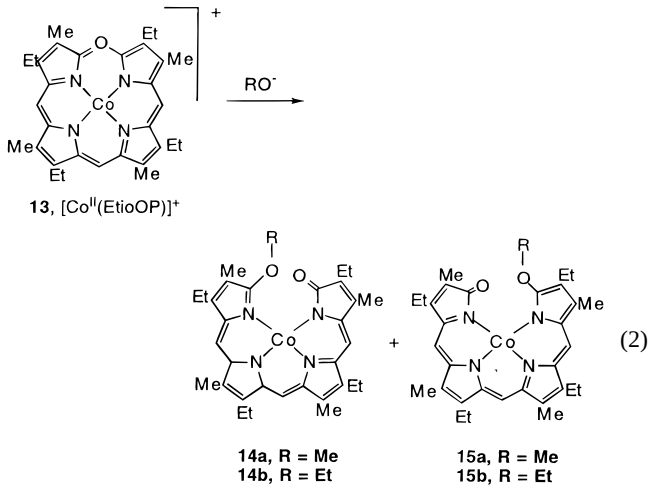

of Figure 4, each of the *meso* resonances appears as a doublet with hyperfine shifts that are similar to those seen for the *meso* protons of **7**. Additionally, six new resonances due to the α-methyl protons of the tetrapyrrole also appear in the spectrum in trace B. The other two α-methyl resonances are probably found in the crowded 10−0 ppm region.

Figure 5 presents data that allow observation of the resonances of the added alkoxide function. Trace A of Figure 5 shows the spectrum of Co^{II}(OEBOEt) that was obtained through the addition of sodium ethoxide in ethanol to a chloroform-*d* solution of [Co^{II}(OEOP)]$^+$. The resonance at −21 ppm is assigned to the methylene protons of the ethoxy group. When ethoxide ion is added to [Co^{II}(EtioOP)]$^+$, **13**, the upfield methylene resonance as well as the downfield *meso* resonances are split into doublets as seen in insets A′ and A″. This doubling of the number of resonances occurs as a result of the formation of two isomeric products as shown in eq 2. Trace B of Figure 5 shows the spectrum that is obtained upon addition of sodium methoxide in methanol to a chloroform-*d* solution of [Co^{II}-(OEOP)]$^+$. The resonance at −100 ppm in the spectrum of the product, Co^{II}(OEBOMe), is due to the protons of the added methoxide group. This resonance is absent from the spectrum of the ethoxy complex that is shown in trace A of Figure 5 and also is absent from the spectra shown in Figure 4 where the solvent and solvent-derived methoxide were deuterated. The effect of addition of sodium methoxide to a sample of Co^{II}-(OEBOEt) in chloroform-*d* is shown in inset B′ in Figure 5. The intensity of the methylene resonance at −22 ppm decreases, while a new resonance due to the methoxy complex grows at −100 ppm. Thus, there is an exchange of the alkoxide group on the tetrapyrrole ligand in Co^{II}(OEBOR) when a different alkoxide is present in the medium.

Three aspects of these alkoxide resonances deserve comment. (1) The methylene resonance of the alkoxy group in Co^{II}-(OEBOEt) appears as a singlet, while all other methylene groups on that tetrapyrrole ligand appear as diastereotopic pairs. This simplification of the spectrum arises from the ready inversion at the oxygen atom which allows the two methylene protons of the ethoxy group to become equivalent. (2) The effect of replacing a proton in Co^{II}(OEBOMe) with a methyl group, as in Co^{II}(OEBOEt), results in a remarkably large difference (ca. 80 ppm) in the chemical shift for the methyl and methylene protons of the alkoxy groups. However, such large differences are observed in other paramagnetic molecules. For example, there is a 127 ppm difference in the chemical shifts of the methyl

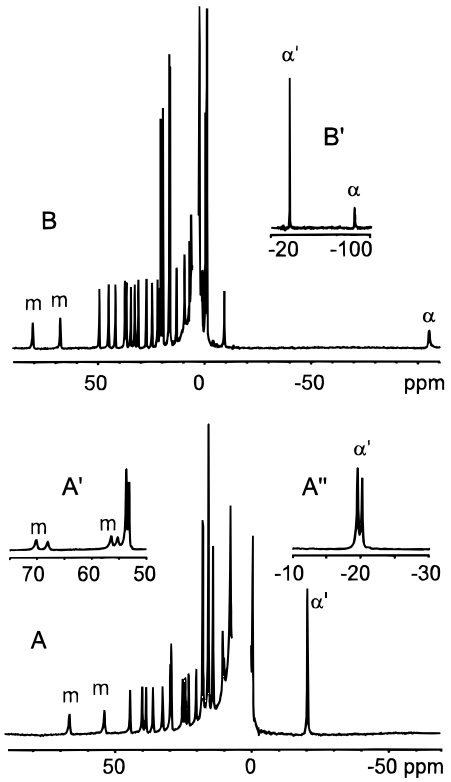

Figure 5. (A) 300 MHz ^{1}H NMR spectrum of Co^{II}(OEBOEt) formed by treating $[Co^{II}(OEOP)](PF_6)$ with potassium ethoxide in chloroform-*d* at 23 °C. Inset A′ shows the *meso* and two pyrrole methyl resonances for Co^{II}(EtioBOEt), while A″ shows the methylene resonances from the ethoxy group in Co^{II}(EtioBOEt). (B) 300 MHz ^{1}H NMR spectrum of Co^{II}(OEBOMe) formed by treating $[Co^{II}(OEOP)](PF_6)$ in chloroform-*d* with sodium methoxide in methanol at 23 °C. Inset B′ shows a portion of the spectrum of Co^{II}(OEBOEt) after the addition of potassium methoxide. The methyl resonances of the methoxy group in Co^{II}(OEBOMe) and the methylene resonances of the ethoxy group in Co^{II}(OEBOEt) are labeled α and α′, respectively, and the resonances from the *meso* protons are labeled m.

resonances in $CH_3CH_2Fe^{III}$(TTP) and the β-methylene resonances in $CH_3CH_2CH_2Fe^{III}$(TTP).[24] (3) The methoxy protons in Co^{II}(OEBOMe) display a remarkably large, upfield hyperfine shift. This large shift probably has its origin in the ability of the oxygen atom of the alkoxy group to facilitate the transmission of spin density from the ligand π-system out onto the methyl group. Similar effects in transmission of spin density have been reported earlier for porphyrin complexes that bear β-pyrrole substituents.[25]

^{1}H NMR spectra nearly identical to those shown in Figures 4A and 5A have been obtained from the addition of cobalt(II) acetate to the free ligand H_2OEBOMe, which is available through treatment of Zn^{II}(OEBOMe) with acid. However, in the absence of excess methoxide, Co^{II}(OEBOMe) is unstable and readily converts to the 5-oxaporphyrin complex, $[Co^{II}(OEOP)]^+$. A method for the preparation and isolation of $[Co^{II}(OEOP)](PF_6)$ from the reaction of cobalt(II) acetate with H_2OEBOMe is given in the Experimental Section.

Figure 6 shows portions of the ^{1}H NMR spectra of Co^{II}(OEBOMe) and Co^{II}(EtioBOMe) in the presence of the chiral alcohol, (*S*)-(+)-2-butanol. As seen in trace A, the low-field *meso* resonances and the upfield methyl resonance of Co^{II}(OEBOMe) appear as doublets with nearly equal intensity when the chiral alcohol is present. These doublets occur because of the diastereomeric differentiation of helical M and P enantiomeric complexes in the chiral environment provided by (*S*)-(+)-2-butanol. It is likely that the added alcohol acts as a ligand and binds to the cobalt ion in these solutions. Trace B shows similar portions of the ^{1}H NMR spectra for Co^{II}(EtioBOMe). Comparison with trace B of Figure 4 shows that 4 rather than 2 *meso* resonances occur in the 70−80 and 60−65 ppm regions. The doubling of signals again is consistent with differentiation of the M and P helical complexes due to interaction with and probable coordination of the chiral alcohol.

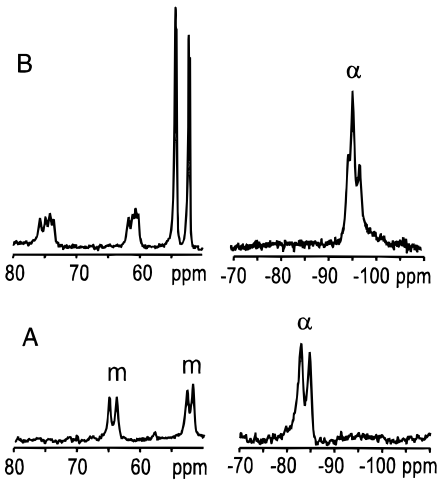

Figure 6. Portions of 300 MHz ^{1}H NMR spectra of (A) Co^{II}(OEBOMe) in chloroform with 2% (*S*)-(+)-2-butanol added and (B) Co^{II}-(EtioBOMe) in chloroform with 2% (*S*)-(+)-2-butanol added.

Reversibility of Reaction 1. Reaction 1 is reversible as shown by the following set of experiments. Addition of methoxide to $[Zn^{II}(OEOP]^+$ yields Zn^{II}(OEBOMe), which may be demetalated through treatment with a weak acid such as dilute acetic acid. The product, H_2OEBOMe, may be isolated as a dark turquoise solid. Cobalt(II) can be inserted into this free ligand to produce Co^{II}(OEBOMe), whose formation can be observed, as described above, by ^{1}H NMR spectroscopy. However, in the absence of an excess of methoxide ion, Co^{II}-(OEBOMe) is easily converted into the verdoheme analogue, $[Co^{II}(OEOP]^+$. Thus treatment of H_2OEBOMe with cobalt(II) acetate in methanol followed by the addition of ammonium hexafluorophosphate in methanol results in the formation of $[Co^{II}(OEOP)](PF_6)$ in greater than 80% isolated yield. However, Zn^{II}(OEBOMe) is much more stable and does not readily form $[Zn^{II}(OEOP]^+$ under comparable conditions.

Discussion

The present study shows that the 5-oxaporphyrin macrocycles in cobalt(II) and zinc(II) complexes undergo addition of alkoxide to produce new complexes that contain the ring-opened tetrapyrrole, alkoxybiliverdin. The formation of the ring-opened cobalt complex, Co^{II}(OEBOMe), is a reversible process. The zinc complexes are sufficiently more stable than their cobalt counterparts so that species such as Zn^{II}(OEBOMe) can be easily isolated and purified. The alkoxybiliverdin ligand assumes a helical geometry in which the alkoxide function and the carbonyl portion of the lactam ring overlap one another. As a consequence, these ligands resemble octaethylbiliverdin and octaethylformylbiliverdin in their coordination geometry. Attempts to isolate Co^{II}(OEBOMe), however, have been unsuccessful due to the ready conversion of Co^{II}(OEBOMe) into the blue-green 5-oxaporphyrin complex, $[Co^{II}(OEOP)]^+$.

(24) Arasasingham, R. D.; Balch, A. L.; Cornman, C. R.; Latos-Grażyński, L. *J. Am. Chem. Soc*. **1989**, *111*, 4357.
(25) Wojaczyński, J.; Latos-Grażyński, L.; Hrycyk, W.; Pacholska, E.; Rachlewicz, K.; Szterenberg, L. *Inorg. Chem.* **1996**, *35*, 6861.

The differentiations observed in the ^{1}H NMR spectra of Co^{II}(OEBOMe) and Co^{II}(EtioBOMe) in the presence of a chiral alcohol, (*S*)-*sec*-butanol, that are shown in Figure 6, are consistent with presence of the M and P helical complexes that interact strongly, probably through coordination, with the alcohol. However, little enantiomeric resolution is observed in these experiments. Previously, it has been shown that Zn^{II}(EtioBOMe) is capable of interacting with amino acid esters so that the L-esters induce M-helicity in the complex.[26]

Experimental Section

Preparation of Compounds. H_3OEB. This compound was prepared via the coupled oxidation of Co^{II}(OEP), as previously reported.[8]

[Zn^{II}(OEOP)](O_2CH_3). The preparation of this compound was adapted from the previous syntheses of zinc(II) α-mesobiliverdin dimethyl ester and zinc(II) 5-oxamesoporphyrin dimethyl ester.[9] H_3OEB (114 mg, 21 mmol) was dissolved in 50 mL of chloroform and heated under reflux. Zinc acetate dihydrate (586 mg, 2.67 mmol) was dissolved in 50 mL of methanol and added to the boiling solution. After 1−2 h, the color of the solution changed from blue to green, which indicated that zinc octaethylbiliverdin, Zn^{II}(HOEB), had formed. After evaporation of the solution to dryness, the crude Zn^{II}(HOEB) was dissolved in a minimum amount of acetic anhydride (∼5 mL) and heated to boiling for 10 min. The solution was cooled to room temperature and poured into 100 mL of chloroform. The resulting solution was washed with water (3 × 200 mL), with saturated sodium bicarbonate (3 × 200 mL), and again with water (3 × 200 mL). The chloroform solution was dried over anhydrous sodium sulfate, filtered, and evaporated to dryness under vacuum. The crude oily solid was dissolved in a minimum volume of chloroform, added to a silica column, and eluted with chloroform. The first band (green) was identified as zinc biliverdin. A second brown band was not identified. The product, [Zn^{II}(OEOP)](O_2CCH_3), was eluted as a blue-green band with 10−20% methanol in chloroform. This fraction was collected and evaporated to dryness. Yield: 84 mg, 62%.

Zn^{II}(OEBOMe). The preparation of this compound was adapted from a previously reported synthesis of zinc 1-methoxy-α-deoxymesobiliverdin dimethyl ester.[10] [Zn^{II}(OEOP)](O_2CCH_3) (66.0 mg, 0.11 mmol) was dissolved in 50 mL of methanol and stirred to give a blue solution. Sodium methoxide (87 mg, 1.60 mmol) was dissolved in 10 mL of methanol and added to the stirred solution. After ca. 1−2 h the reaction was complete, and a green/yellow solution of Zn^{II}(OEBOMe) had formed. The methanol solution was then poured into 100 mL of dichloromethane, washed with water (3 × 200 mL), dried on anhydrous sodium sulfate, and evaporated to dryness. Yield: 61.1 mg, 90%. UV/vis spectrum in chloroform [λ_{max}, nm, (ϵ, M^{-1} cm^{-1})]: 322 (22 300), 402 (33 600), 790 (16 000). 300 MHz ^{1}H NMR (chloroform-*d*): δ = 6.45 (s, 1 H, meso proton), 6.44 (s, 1 H, meso proton), 5.47 (s, 1H, meso proton), 4.25 (s, 3 H, methoxy protons), 2.43 (m, 12 H, methylene protons), 2.15 (m, 4 H, methylene protons), 1.13 (m, 12 H, methyl protons), 0.97 (m, 12 H, methyl protons). Infrared spectrum (Fluorolube mull): 2968, 2936, 2873, 1658, 1606, 1576, 1535, 1523 1466, 1454, 1396, 1382 cm^{-1}.

H_2OEBOMe. Zn^{II}(OEBOMe) (25 mg. 0.04 mmol) was dissolved in 50 mL of dichloromethane and shaken vigorously with 150 mL of 0.5% (v/v) aqueous acetic acid (pH ∼ 4−6) for approximately 2 min or until a deep turquoise-blue color appeared. The dichloromethane layer was separated, diluted with 50 mL dichloromethane, washed with water (3 × 150 mL), dried with anhydrous sodium sulfate, and evaporated to dryness under vacuum. The solid residue was subjected to column chromatography on silica gel with dichloromethane as eluant. The first blue band (there is a second blue band that contains H_3OEB) was collected and evaporated to dryness. Yield: 14.7 mg, 65%. UV/vis in chloroform [λ_{max}, nm (ϵ, M^{-1} cm^{-1})]: 304 (22 700), 372 (50 900), 672 (18 100). 300 MHz ^{1}H NMR (chloroform-*d*): δ = 13.01 (br s, 1 H, N−H), 10.29 (br s, 1 H, N−H), 6.60 (s, 1 H, meso proton), 6.27 (s, 1 H, meso proton), 5.74 (s, 1H, meso proton), 4.01 (s, 3 H, methoxy protons), 2.49 (m, 12 H, methylene protons), 2.20 (m, 4 H, methylene protons), 1.10 (m, 24 H, methyl protons).

Table 2. Crystal Data and Data Collection Parameters for Zn^{II}(OEBOMe)

formula	$C_{36}H_{46}N_4O_2Zn$
fw	632.14
color and habit	dark green needles
cryst system	triclinic
space group	$P\bar{1}$
a, Å	10.345(2)
b, Å	13.844(3)
c, Å	13.863(3)
α, deg	113.20(3)
β, deg	101.37(3)
γ, deg	107.37(3)
V, Å^3	1625.7(6)
T, K	130(2)
Z	2
d_{calcd}, g cm^{-3}	1.291
radiation (*λ*, Å)	Cu Kα (1.541 78)
μ, mm^{-1}	1.336
range of transm factors	0.52−0.72
no. of unique data	4388
no. of params refined	397
R^a	0.049
w$R2^b$	0.142

^{a} $R = \sum||F_o| - |F_c||/\sum|F_o|$ (observed data, $I > 2\sigma(I)$). ^{b} w$R2 = [\sum[w(F_o^2 - F_c^2)^2]/\sum[w(F_o^2)^2]]^{1/2}$ (all data).

Methoxide Additions to [Co^{II}(OEOP)](PF_6). All samples of [Co^{II}(OEOP)](PF_6),[8] Co^{II}(OEBOMe), and methoxide solutions were prepared and sealed in dioxygen-free solvents under a dinitrogen atmosphere in a glovebox. Solutions of sodium methoxide were produced by saturating a methanol solution with solid sodium methoxide. Solutions of sodium methoxide-d_3 were prepared by dissolution of 100 μL of 40 wt % KOD/D_2O in 2 mL of methanol-d_4. Reactions with either methoxide source produced similar results, but the addition of sodium methoxide introduces an overwhelming ^{1}H NMR signal from the added methoxide. NMR titrations with these methoxide solutions into a septum sealed NMR tube that contained a solution of the appropriate cobalt complex were performed with a 10 or 100 μL syringe. Sample concentrations for [Co^{II}(OEOP)](PF_6) were on the order of 1−3 mM and typically required 2−20 μL of methoxide solution for complete conversion. ^{1}H NMR (*δ*, ppm in chloroform-*d* at 23 °C for Co^{II}(OEBOMe): *meso* protons, 78.0, 64.0, −7.0; methylene protons, 46.6, 44.9, 40.3, 38.3, 34.6, 33.2, 31.9, 30.7, 25.6, 24.6, 22.9, 18.8, 14.1, 8.3 (double intensity), 5.7; methyl protons, 19.4, 18.2, 17.3, 16.4, 1.8, 0.9, 0.0, −1.1; methoxy protons, −101.6 ppm.

[Co^{II}(OEOP)](PF_6) from Co^{II}(OEBOMe). A sample of 25.1 mg (0.04 mmol) of H_2OEBOMe was dissolved in 10 mL of methanol. Cobalt(II) acetate tetrahydrate (11.5 mg, 0.04 mmol) was added to this solution. The electronic absorption spectrum of the greenish-yellow solution revealed that Co^{II}(OEBOMe) had formed. After the solution was heated to 50 °C for 5 min, it turned deep blue which is the color of [Co^{II}(OEOP)]$^+$. Ammonium hexafluorophosphate (36.0 mg, 0.22 mmol) was added to the mixture, which was stirred for 5 min. The solution was evaporated to dryness. The residue was dissolved in a minimum volume of dichloromethane, and the solution was filtered. The filtrate was evaporated to dryness, and the solid was recrystallized from dichloromethane/hexane. Yield: 27.1 mg, 83%. The purple microcrystalline solid was identified as [Co^{II}(OEOP)](PF_6) by spectroscopic comparison with an authentic sample.[8]

X-ray Data Collection for Zn^{II}(OEBOMe). Crystals were obtained by layering an acetone solution of Zn^{II}(OEBOMe) over a layer of water in a 5 mm glass tube. Slow diffusion of water into the acetone solution of the complex produced green needles. A needle was coated with a light hydrocarbon oil and mounted in the 130 K dinitrogen stream of a Syntex $P2_1$ diffractometer equipped with a locally modified low-temperature apparatus. Intensity data were collected using graphite-monochromated Cu Kα radiation. Crystal data are given in Table 2.

(26) Mizutani, T.; Yagi, S.; Honmaru, A.; Ogoshi, H. *J. Am. Chem. Soc*. **1996**, *118*, 5318.

Two check reflections showed only random (<1%) variation in intensity during data collection. The data were corrected for Lorentz and polarization effects. Further details are given in the Supporting Information.

Solution and Structure Refinement. Calculations were performed with SHELXTL 5 series of programs Scattering factors and correction for anomalous dispersion were taken from a standard source.[27] An absorption correction was applied.[28] The solution was determined by direct methods and subsequent cycles of least-squares refinement and calculation of difference Fourier maps.

Instrumentation. ^{1}H NMR spectra were recorded on a General Electric QE-300 FT NMR spectrometer operating in the quadrature mode (^{1}H frequency is 300 MHz). The spectra of paramagnetic molecules were collected over a 50 kHz bandwidth with 16 K data points and a 5 μs 90° pulse. For a typical spectrum, between 1000 and 5000 transients were accumulated with a 50 ms delay time. The signal-to-noise ratio was improved by apodization of the free inducing decay. Electronic spectra were obtained using a Hewlett-Packard diode array spectrometer.

Acknowledgment. We thank the NIH (Grant GM-26226) for financial support and Richard Koerner for helpful discussions.

Supporting Information Available: X-ray crystallographic files, in CIF format, for Zn^{II}(OEBOMe) are available on the Internet only. Access information is given on any current masthead page.

IC971584H

(27) *International Tables for Crystallography*; Wilson, A. J. C., Ed.; Kluwer Academic Publishers: Dordrecht, The Netherlands, 1992; Vol. C.
(28) Parkin, S.; Moezzi, B.; Hope, H. *J. Appl. Crystallogr.* **1995**, *28*, 53.